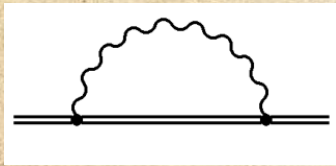


CALCULATIONS OF QED CORRECTIONS WITH DIRAC GREEN FUNCTION

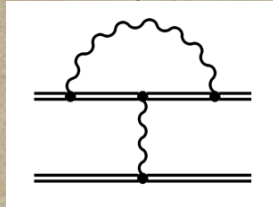
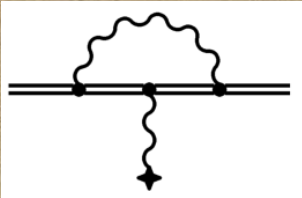
Vladimir A. Yerokhin

EMMI workshop, 26 October 2022, Sorbonne, Paris

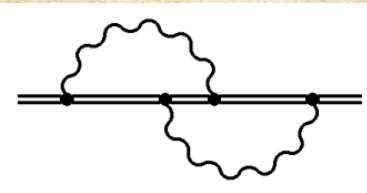
Electron self-energy QED corrections: the zoo



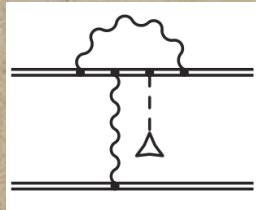
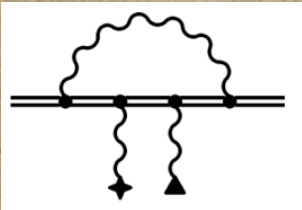
From 1974, *Mohr, Indelicato, Jentschura,...*



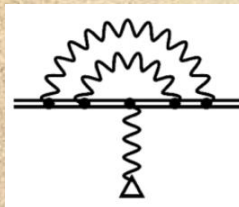
From 1996, *Persson, Blundell, Yerokhin, Sapirstein,...*



From 2001, *Yerokhin, Shabaev, Indelicato*

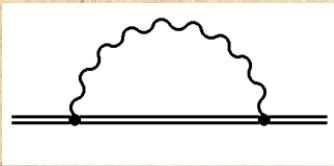


From 2005, *Shabaev, Glazov, Volotka, Yerokhin,...*



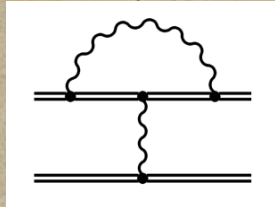
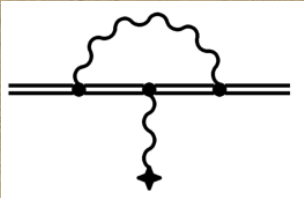
still in progress ...

Electron self-energy QED corrections: the zoo



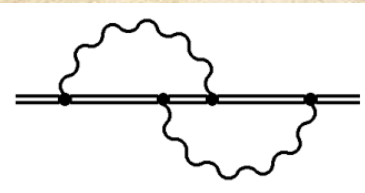
From 1974, Mohr, Indelicato, Jentschura,...

Need for a technique that
allows to compute various
QED corrections in a
standardized way.

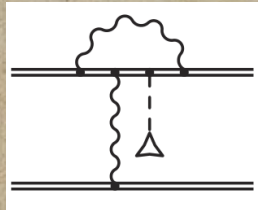
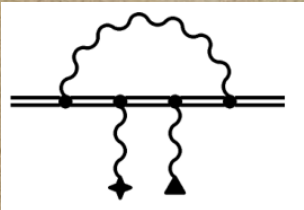


From :

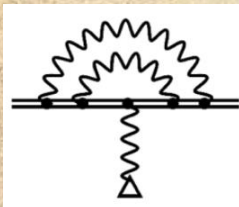
Sapirstein,...



From 2001, Yerokhin, Shabaev, Indelicato

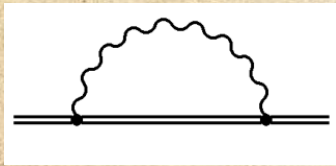


From 2005, Shabaev, Glazov, Volotka, Yerokhin,...



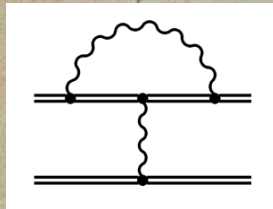
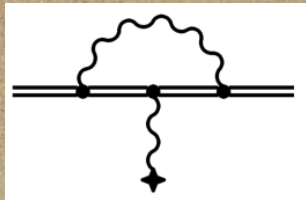
still in progress ...

Electron self-energy QED corrections: the zoo



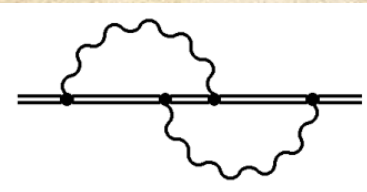
From 1974, Mohr, Indelicato, Jentschura,...

Need for a technique that allows to compute various QED corrections in a standardized way



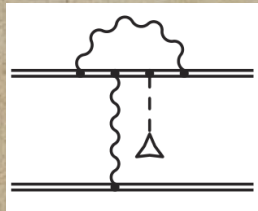
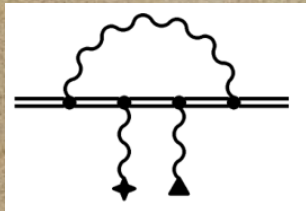
From :

Sapirstein,...



From 2001

Wish list:
☐ Without expansion in the electron-nucleus binding strength (parameter $Z\alpha$).

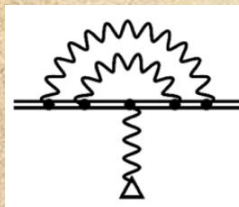


From 2005

☐ For general binding potential (not only Coulomb).

☐ "Arbitrary" number of radial integrations.

n,...



still in progress ...

Reading Feynman diagrams

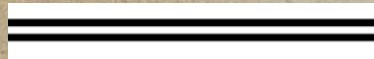
Internal photon line



Photon propagator

$$g^{\mu\nu} \frac{i\omega}{4\pi} \sum_l (2l+1) j_l(\omega x_<) h_l^{(1)}(\omega x_>) P_l(\hat{x}_1 \cdot \hat{x}_2)$$

External electron line



Dirac bound-state wave function

$$\psi_a(\mathbf{x})$$

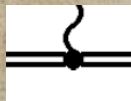
Internal electron line



Bound electron propagator (= Dirac Green function)

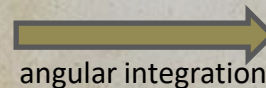
$$\sum_{\kappa=\pm 1}^{\pm\infty} G_{\kappa}(E, x_1, x_2) \circ \Pi_{\kappa}(\hat{x}_1, \hat{x}_2)$$

Vertex



Integration over the coordinate

$$\int d^3x$$



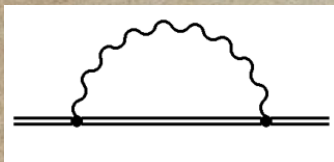
angular integration

$$\int_0^{\infty} x^2 dx$$

Closed loop

Integration over loop frequency

E.g.:



Two radial integrations, one loop frequency integration, two wave functions, one photon propagator, one electron propagator + one partial wave expansion.

Dirac Green function

Representation via regular/irregular Dirac solutions

$$G_{\kappa}(E, x, x') = \phi_{\kappa}^{\infty}(E, x) \phi_{\kappa}^{0^T}(E, x') \theta(x - x') \\ + \phi_{\kappa}^0(E, x) \phi_{\kappa}^{\infty^T}(E, x') \theta(x' - x),$$

$\phi_{\kappa}^0(x)$ -- Dirac solution regular at the origin

$\phi_{\kappa}^{\infty}(x)$ -- Dirac solution regular at the infinity



High numerical accuracy,
high partial waves accessible.



More difficult to work with.

Spectral representation Finite basis sets

$$G_{\kappa}(E, x, x') = \sum_n \frac{\phi_{\kappa,n}(x) \phi_{\kappa,n}^T(x')}{E - \varepsilon_{\kappa,n}},$$

B-spline finite basis set method

[Johnson et al., PRA 37, 305 (1988)]

Dual Kinetic Balance B-spline basis set

[Shabaev et al., PRL 93, 130405 (2004)]



Robustness, flexibility,
convenient to work with.



Convergence with respect to
the basis size; high partial waves
are not accessible.

Regular and irregular Dirac solutions

$$\phi^0(x) = \begin{pmatrix} \phi_+^0(x) \\ \phi_-^0(x) \end{pmatrix}, \quad \phi^\infty(x) = \begin{pmatrix} \phi_+^\infty(x) \\ \phi_-^\infty(x) \end{pmatrix},$$

For the pure Coulomb potential:

Wichmann and Kroll, PR 101, 843 (1956),
P.J. Mohr, Ann. Phys. 88, 26 (1974).

$$\begin{aligned} \phi_\pm^0(x) &= \Delta_\kappa^{-1/2} \frac{\sqrt{1 \pm \varepsilon}}{x^{3/2}} \left[(\lambda - \nu) M_{\nu-(1/2), \lambda}(2cx) \mp \left(\kappa - \frac{\alpha Z}{c} \right) M_{\nu+(1/2), \lambda}(2cx) \right], \\ \phi_\pm^\infty(x) &= \Delta_\kappa^{-1/2} \frac{\sqrt{1 \pm \varepsilon}}{x^{3/2}} \left[\left(\kappa + \frac{\alpha Z}{c} \right) W_{\nu-(1/2), \lambda}(2cx) \pm W_{\nu+(1/2), \lambda}(2cx) \right], \end{aligned}$$

where $\Delta_\kappa = -4c^2 \frac{\Gamma(1+2\lambda)}{\Gamma(\lambda-\nu)}$, $\varepsilon = E/m$, $c = \sqrt{1 - \varepsilon^2}$, $\lambda = \sqrt{\kappa^2 - (\alpha Z)^2}$, $\nu = Z\alpha\varepsilon/c$.

For the general (asymptotically Coulomb) potential:

Power-series solution of the Dirac equation on a radial grid.

[Yerokhin, PRA 83, 012507 (2011); Salvat and Fernández-Varea, CPC 90, 151 (1995)].

Note: For the Coulomb potential, the Dirac functions can be calculated at a given radial point. For the general potential, calculation has to be carried out for the whole radial grid.

Radial integrations with Dirac Green function: difficulties and advantages

$$G_{\kappa}(E, x, x') = \phi_{\kappa}^{\infty}(E, x) \phi_{\kappa}^{0^T}(E, x') \theta(x - x') \\ + \phi_{\kappa}^0(E, x) \phi_{\kappa}^{\infty^T}(E, x') \theta(x' - x),$$

Care needs to be taken of:

- ❑ Discontinuity at $x = x'$.
- ❑ Dominant contribution from the region $x \approx x'$,
- ❑ Exponential/powerlike growth/decrease of Dirac solutions at origin and infinity.

$$\phi_{\kappa}^0(\varepsilon, x) = x^{|\kappa|} e^{\sqrt{1-\varepsilon^2}x} \tilde{\phi}_{\kappa}^0(\varepsilon, x), \\ \phi_{\kappa}^{\infty}(\varepsilon, x) = x^{-|\kappa|} e^{-\sqrt{1-\varepsilon^2}x} \tilde{\phi}_{\kappa}^{\infty}(\varepsilon, x).$$

Advantages to be used:

- ❑ Semi-factorization of radial variables.
("semi" because of the radial ordering.)

It is sufficient to know Dirac solutions on a one-dimensional radial grid, in order to obtain the Green function on a two-dimensional radial grid!

Computation of multiple radial integrals with Dirac Green function

A (simplest) example, two-dimensional radial integral:

$$\int_0^\infty dx \int_0^\infty dx' H(x) I(x_<) L(x_>) M(x') = \int_0^\infty dx \left(\int_0^x dx' + \int_x^\infty dx' \right) H(x) I(x_<) L(x_>) M(x').$$

Numerical integration = some quadrature formula:

$$\int_0^\infty dx f(x) = \sum_{i=1}^N w_i f(x_i) = \sum_{i=1}^N w_i \left(\int_0^{x_i} dx' + \int_{x_i}^\infty dx' \right) g(x_i) h(x').$$

$$\{x_i\}_{i=1}^N$$

Quadrature grid for the outermost radial integral

$$x_{i,j} \in (x_i, x_{i+1})$$

Finer quadrature grid for the second integral

$$x_{i,j,k} \in (x_{i,j}, x_{i,j+1})$$

Even finer grid for the third integral

...

Any number of integrations can be accommodated ...

For arbitrary number of radial integrations, all functions in the integrand need to be stored only on a one-dimensional grid !

Computation of multiple radial integrals with Dirac Green function

The procedure:

- ❑ Set up the (1-dimensional) radial grid,
- ❑ Store all wave functions/Dirac solutions for Green functions/Bessel functions for photon propagators on this radial grid,
- ❑ Perform all radial integrations by summing up the pre-stored values.

Advantages:

- ❑ Simple and robust, easy to implement,
- ❑ Computation of Dirac Green function takes only a small part of computation time (possible to switch to quadruple arithmetics with no extra costs),
- ❑ The same procedure for the point Coulomb potential and the general potential.

Disdvantages:

- ❑ Not the most effective way possible; a relative large number of integration points is required.

Computation of multiple radial integrals with Dirac Green function

4-fold radial integrations with Dirac Green function appeared in:

- ❑ Two-loop self-energy [Yerokhin et al., PRL 91, 073001 (2003); PRL 97, 253004 (2006), ...],
- ❑ Self-energy for nuclear magnetic shielding [Yerokhin et al., PRL 107, 043004 (2011)],
- ❑ Self-energy screening for g factor [Yerokhin et al., PRA 102, 022815 (2020)].

5-fold radial integrations:

- ❑ Two-loop self-energy for g factor [in progress].

Conclusions

- ❑ Calculations with Dirac Green function are not that hard !
- ❑ Multiple radial integrations in various QED corrections with Dirac Green functions can be computed within the same approach [usually the most numerically-intensive part].
- ❑ Separation of ultraviolet and infrared divergencies (and computation of finite remaining parts) are individual for different QED corrections.



symmetry

2020, 12, 800; doi:10.3390/sym12050800

Review

Calculations of QED Effects with the Dirac Green Function

Vladimir A. Yerokhin * and Anna V. Maierova

Model QED operator

PHYSICAL REVIEW A **106**, 012806 (2022)

Model-QED operator for superheavy elements

A. V. Malyshev¹, D. A. Glazov¹, V. M. Shabaev¹, I. I. Tupitsyn¹, V. A. Yerokhin², and V. A. Zaytsev¹

¹*Department of Physics, St. Petersburg State University, Universitetskaya 7/9, 199034 St. Petersburg, Russia*

²*Peter the Great St. Petersburg Polytechnic University, Polytekhnicheskaya 29, 195251 St. Petersburg, Russia*



(Received 23 April 2022; accepted 22 June 2022; published 12 July 2022)

The model-QED-operator approach [V. M. Shabaev, I. I. Tupitsyn, and V. A. Yerokhin, *Phys. Rev. A* **88**, 012513 (2013)] to calculations of the radiative corrections to binding and transition energies in atomic systems is extended to the range of nuclear charges $110 \leq Z \leq 170$. The self-energy part of the model operator is represented by a nonlocal potential based on diagonal and off-diagonal matrix elements of the *ab initio* self-energy operator with the Dirac-Coulomb wave functions. The vacuum-polarization part consists of the Uehling contribution, which is readily computed for an arbitrary nuclear-charge distribution and the Wichmann-Kroll contribution represented in terms of matrix elements similarly to the self-energy part. The performance of the method is studied by comparing the model-QED-operator predictions with the results of *ab initio* calculations. The model-QED operator can be conveniently incorporated in any numerical approach based on the Dirac-Coulomb-Breit Hamiltonian to account for the QED effects in a wide variety of superheavy elements.

DOI: [10.1103/PhysRevA.106.012806](https://doi.org/10.1103/PhysRevA.106.012806)

QED calculations with hydrogenic wave functions

$$\langle i | \Sigma_{SE} | k \rangle = \frac{\alpha}{\pi} \frac{(\alpha Z)^4}{(n_i n_k)^{3/2}} F_{n_i n_k}(\alpha Z) m c^2.$$

S-states:

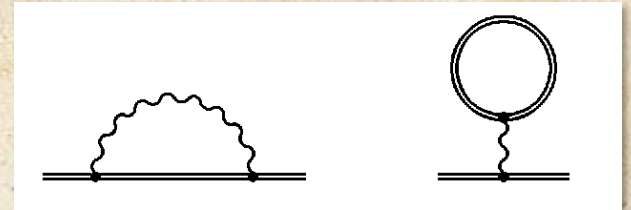
Z	R	(1,1)	(1,2)	(1,3)	(1,4)	(1,5)	(2,2)	(2,3)	(2,4)	(2,5)	(3,3)	(3,4)	(3,5)	(4,4)	(4,5)	(5,5)
110	6.188	1.5744	1.9995	1.9788	1.9353	1.9006	2.6283	2.6172	2.5695	2.5278	2.6009	2.5505	2.5104	2.4980(1)	2.4559(1)	2.4137(5)
115	6.291	1.6401	2.1172	2.0862	2.0322	1.9901	2.8439	2.8170	2.7535	2.7008	2.7882	2.7215	2.6704	2.6547(1)	2.6015(1)	2.5492(4)
120	6.391	1.7275	2.2666	2.2210	2.1532	2.1015	3.1127	3.0636	2.9790	2.9117	3.0174	2.9296	2.8639	2.8440(1)	2.7769(1)	2.7117(4)
125	6.494	1.8402	2.4519	2.3854	2.2994	2.2354	3.4427	3.3621	3.2490	3.1625	3.2917	3.1762	3.0916	3.0663(1)	2.9815(1)	2.9001(3)
130	6.588	1.9832	2.6774	2.5809	2.4709	2.3911	3.8397	3.7149	3.5634	3.4518	3.6109	3.4597	3.3507	3.3184	3.2116(1)	3.1099(3)
135	6.691	2.1596	2.9412	2.8026	2.6615	2.5619	4.2976	4.1118	3.9099	3.7663	3.9627	3.7663(1)	3.6268	3.5859	3.4525(1)	3.3262(2)
140	6.785	2.3728	3.2372	3.0417	2.8616	2.7380	4.7978	4.5315	4.2662	4.0835	4.3250	4.0743(1)	3.8982	3.8474	3.6832(1)	3.5285(2)
145	6.883	2.6203	3.5445	3.2777	3.0518	2.9007	5.2928	4.9293	4.5900	4.3628	4.6570(1)	4.3459(1)	4.1293	4.0680(1)	3.8711(1)	3.6860(2)
150	6.983	2.8941	3.8316	3.4851	3.2099	3.0298	5.7178	5.2514	4.8341	4.5612	4.9159(1)	4.5442(1)	4.2866	4.2160(1)	3.9875(1)	3.7732(1)
155	7.075	3.1808	4.0637	3.6414	3.3182	3.1102	6.0137	5.4569	4.9665	4.6514	5.0765(1)	4.6504(1)	4.3556	4.2785(1)	4.0227(1)	3.7830(1)
160	7.170	3.4565	4.2051	3.7273	3.3632	3.1312	6.1433	5.5273	4.9772	4.6278	5.1351(1)	4.6664(1)	4.3411	4.2614(1)	3.9842(1)	3.7247(1)
165	7.268	3.6964	4.2393	3.7385	3.3445	3.0944	6.1212	5.4837	4.8897	4.5151	5.1181(1)	4.6186(1)	4.2697	4.1913(1)	3.8982(1)	3.6243(1)
170	7.358	3.8831	4.1722	3.6850	3.2731	3.0108	6.0026	5.3717	4.7466	4.3539	5.0656	4.5433	4.1759	4.1013(1)		

D_{5/2}-states:

Z	R	(3,3)	(3,4)	(3,5)	(4,4)	(4,5)	(5,5)
110	6.188	0.0699	0.0672	0.0642	0.0783(1)	0.0786(1)	0.0825(5)
115	6.291	0.0722	0.0695	0.0665	0.0812(1)	0.0816(1)	0.0856(4)
120	6.391	0.0745	0.0719	0.0688	0.0842	0.0846(1)	0.0888(4)
125	6.494	0.0769	0.0743	0.0711	0.0871	0.0876(1)	0.0921(3)
130	6.588	0.0793	0.0767	0.0735	0.0902	0.0908(1)	0.0954(3)
135	6.691	0.0817	0.0792	0.0758	0.0933	0.0939(1)	0.0988(2)
140	6.785	0.0842	0.0818	0.0783	0.0965	0.0972(1)	0.1023(2)
145	6.883	0.0868	0.0845	0.0809	0.0999	0.1008(1)	0.1061(2)
150	6.983	0.0896	0.0874	0.0837	0.1036	0.1046(1)	0.1102(2)
155	7.075	0.0926	0.0906	0.0868	0.1076	0.1088(1)	0.1147(1)
160	7.170	0.0958	0.0940	0.0902	0.1120	0.1134	0.1196(1)
165	7.268	0.0991	0.0977	0.0938	0.1166	0.1183	0.1249(1)
170	7.358	0.1026	0.1014	0.0976	0.1215	0.1234	0.1304(1)

S, P_{1/2}, P_{3/2},
D_{3/2}, D_{5/2}
states are
calculated

Model QED operator approach



Non-local model QED operator:

$$h^{\text{QED}} = \sum_{ijlk=1}^n |\phi_i\rangle (D^{-1})_{ji} \left\langle \psi_j \left| \left[\frac{1}{2} \Sigma(\varepsilon_j) + \frac{1}{2} \Sigma(\varepsilon_l) + V_{\text{VP}} \right] \right| \psi_l \right\rangle (D^{-1})_{lk} \langle \phi_k|,$$

where

$\Sigma(\varepsilon)$ is the exact one-loop self-energy operator,

V_{VP} is the vacuum-polarization potential,

ψ_i are the hydrogenic wave functions,

ϕ_i are the model wave functions,

and D is the overlap matrix, $D_{ij} = \langle \phi_i | \psi_j \rangle$.

No fitting is involved!

Model QED versus Exact QED

TABLE I. Self-energy correction for the valence ns electrons in the alkali-metal-like configurations $[\text{Ne}]3s$, $[\text{Ne}]3s^23p^64s$, and $[\text{Ne}]3s^23p^63d^{10}4s^24p^65s$.

Z	Approach	$3s$	$4s$	$5s$
110	Exact	2.249	1.925	1.389
	Mod. op.	2.251	1.927	1.393
	H-like	2.601	2.498	2.414
120	Exact	2.640	2.242	1.650
	Mod. op.	2.642	2.247	1.656
	H-like	3.017	2.844	2.712
130	Exact	3.193	2.670	1.985
	Mod. op.	3.194	2.677	1.993
	H-like	3.611	3.318	3.110
140	Exact	3.862	3.154	2.349
	Mod. op.	3.863	3.162	2.357
	H-like	4.325	3.847	3.528
150	Exact	4.433	3.516	2.605
	Mod. op.	4.433	3.519	2.608
	H-like	4.916	4.216	3.773
160	Exact	4.666	3.597	2.644
	Mod. op.	4.672	3.597	2.640
	H-like	5.135	4.261	3.725
170	Exact	4.613	3.479	2.536
	Mod. op.	4.635	3.479	2.528
	H-like	5.066	4.101	3.511

THANK YOU
FOR
YOUR ATTENTION